REPORT DOCUMENTATION PAGE

Form Approved OMB NO. 0704-0188

1. REPORT DATE (DD-MM-YYYY)	2. REPORT TYPE	3. DATES COVERED (From - To)
	New Reprint	-

4. TITLE AND SUBTITLE
Robust SERS Enhancement Factor Statistics Using Rotational Correlation Spectroscopy

5a. CONTRACT NUMBER

5b. GRANT NUMBER
W911NF-09-D-0001

5c. PROGRAM ELEMENT NUMBER
611104

6. AUTHORS
Ted A. Laurence, Gary B. Braun, Norbert O. Reich, Martin Moskovits

5d. PROJECT NUMBER

5e. TASK NUMBER

5f. WORK UNIT NUMBER

7. PERFORMING ORGANIZATION NAMES AND ADDRESSES
University of California - Santa Barbara
3227 Cheadle Hall
3rd floor, MC 2050
Santa Barbara, CA 93106 -2050

8. PERFORMING ORGANIZATION REPORT NUMBER

9. SPONSORING/MONITORING AGENCY NAME(S) AND ADDRESS(ES)
U.S. Army Research Office
P.O. Box 12211
Research Triangle Park, NC 27709-2211

10. SPONSOR/MONITOR'S ACRONYM(S)
ARO

11. SPONSOR/MONITOR'S REPORT NUMBER(S)
55012-LS-ICB.597

12. DISTRIBUTION AVAILIBILITY STATEMENT
Approved for public release; distribution is unlimited.

13. SUPPLEMENTARY NOTES
The views, opinions and/or findings contained in this report are those of the author(s) and should not contrued as an official Department of the Army position, policy or decision, unless so designated by other documentation.

14. ABSTRACT
See attached.

15. SUBJECT TERMS
See attached.

16. SECURITY CLASSIFICATION OF:			17. LIMITATION OF ABSTRACT	15. NUMBER OF PAGES	19a. NAME OF RESPONSIBLE PERSON
a. REPORT	b. ABSTRACT	c. THIS PAGE			Francis Doyle
UU	UU	UU	UU		19b. TELEPHONE NUMBER: 805-893-8133

Report Title

Robust SERS Enhancement Factor Statistics Using Rotational Correlation Spectroscopy

ABSTRACT

See attached.

REPORT DOCUMENTATION PAGE (SF298)
(Continuation Sheet)

Continuation for Block 13

ARO Report Number 55012.597-LS-ICB
Robust SERS Enhancement Factor Statistics Us ...

Block 13: Supplementary Note

Approved for public release; distribution is unlimited.

NANO LETTERS

Letter

pubs.acs.org/NanoLett

Robust SERS Enhancement Factor Statistics Using Rotational Correlation Spectroscopy

Ted A. Laurence,*[,†,§] Gary B. Braun,[‡,§] Norbert O. Reich,[‡] and Martin Moskovits[‡]

[†]Physical and Life Sciences Directorate, Lawrence Livermore National Laboratory, Livermore, California 94550, United States

[‡]Department of Chemistry and Biochemistry, University of California, Santa Barbara, California 93106, United States

Supporting Information

ABSTRACT: We characterize the distribution of surface-enhanced Raman spectroscopy (SERS) enhancement factors observed in individual hot spots of single Ag "nanocapsules", encapsulated Ag nanoparticle dimers formed via controlled nanoparticle linking, polymer encapsulation, and small molecule infusion. The enhancement factors are calculated for over 1000 individual nanocapsules by comparing Raman scattering intensities of 4-mercaptobenzoic acid (MBA) measured from single SERS hot spots to intensities measured from high-concentration solutions of MBA. Correlation spectroscopy measurements of the rotational diffusion identify nanocapsules with signals dominated by single hot spots via their strong polarization response. Averaging over the entire surface of the nanocapsules, the distribution of enhancement factors is found to range from 10^6 to 10^8, with a mean of 6×10^6. Averaging only over nanoparticle junctions (where most SERS signals are expected) increases this average value to 10^8, with a range from 2×10^7 to 2×10^9. This significant statistical sampling shows that very high SERS enhancement factors can be obtained on a consistent basis using nanoparticle linking.

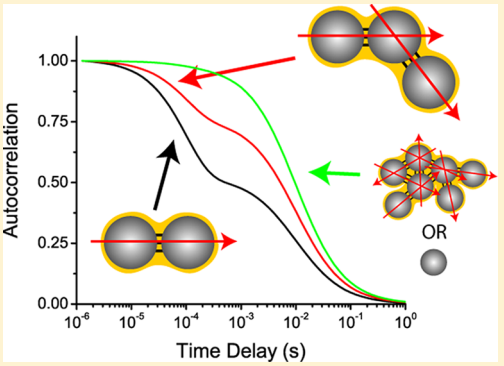

KEYWORDS: *Surface-enhanced Raman scattering, localized surface plasmons, metallic nanoparticles, single particle spectroscopy, correlation spectroscopy*

An objective of many current surface-enhanced Raman spectroscopy (SERS) studies is to obtain more highly and more uniformly enhancing SERS substrates facilitating quantitative, analytical applications. Recently, we reported a SERS substrate (that we dubbed "SERS nanocapsules") consisting of encapsulated nanoparticle dimers as its major component, which were produced by a controlled linking and passivation scheme. These nanocapsules exhibited strong, uniform SERS signals.[1−4] Wustholz et al. have used a similar approach to obtain consistent enhancement factors (EFs) correlating nanoparticle aggregate geometry determined from electron microscopy with SERS for Au.[5] We also reported a methodology for rapidly characterizing the SERS intensity distribution of individual hot spots by comparing the intensities from nanoparticles diffusing in solution.[2] More recently, methodological approaches have been reported for measuring entire spectra of flowing, individual nanoparticle clusters with high signal-to-noise.[6]

Here, we develop a quantitative technique for analyzing SERS colloidal substrates based on determining the orientationally averaged intensity of those nanoparticle dimers or multimers for which the contribution of single dimer hot spots can be unequivocally determined. The strength and distribution of the enhancement factors are obtained from the ensemble of individual Ag SERS nanocapsules freely diffusing in solution, which were produced and loaded with 4-mercaptobenzoic acid (MBA) as described previously (Figure 1A).[1−3]

We measure the enhancement factors for a large number of nanocapsules by comparing the Raman scattering from high-concentration solutions of MBA and the SERS signal of MBA from diffusing nanocapsules (Figure 1B). The Raman lines near 1100 and 1600 cm^{-1} shift by ∼15 cm^{-1} on going from the normal Raman spectrum of MBA to the SERS measurements, most likely due to the formation of a Ag^+S^- coordinative bond.[7]

We calculate enhancement in two ways. First, we use the SERS substrate enhancement factor (SSEF) suggested by Le Ru et al.,[8] applied to individual SERS nanocapsules by calculating the average surface area of a nanocapsule. We also calculate the average enhancement over all molecules resident in the hotspot of a single nanocapsule by estimating hot spot areas as the contact areas between nanoparticles. We call this the hot spot enhancement factor (HSEF). The nanocapsules were exposed to enough MBA to allow the molecule to saturate all of the available binding sites. Averaging over the entire surface of the nanocapsules, the distribution of enhancement factors is found to range from 10^6 and 10^8, with a mean of 6×10^6. Averaging only over nanoparticle junctions (where most SERS signal is expected) increases this average value to 10^8, with a range from 2×10^7 to 2×10^9.[5,8−10] These results are compared to samples immobilized on a glass coverslip.

Received: February 8, 2012
Revised: April 28, 2012
Published: May 2, 2012

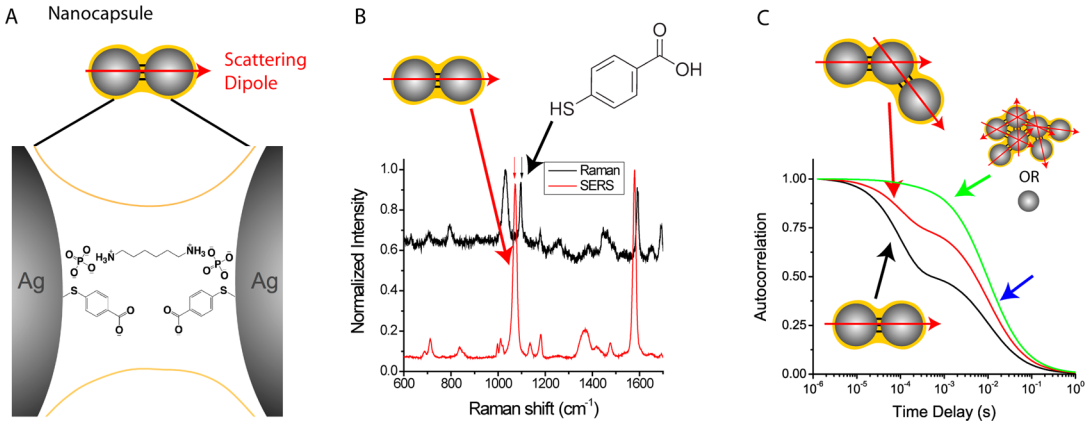

Figure 1. (A) Schematic of the junction of nanocapsules formed using bifunctional groups to link nanoparticles. Polymer coatings quench the reaction, preventing further aggregation when a Raman active molecule is added. (B) The bulk Raman spectrum of MBA in methanol and the SERS spectrum of MBA are shown. Note the change in the Raman shift for the ring breathing mode of MBA between bulk Raman and SERS (some methanol Raman lines are visible in the bulk MBA spectrum). (C) We verify that the measured enhancement factors are for individual hot spots by monitoring the polarization-induced rotational diffusion fluctuations. SERS correlation spectroscopy reveals two time scales as shown in this schematic: one from translational diffusion (blue arrow) and another from rotational diffusion (black, red, and green arrows). The ratio of the amplitude of the rotational diffusion component to the translational diffusion component depends on the number of possible scattering dipole orientations and hence on the aggregation state of the nanoparticles. Single dipoles have the strongest polarization-induced correlation amplitude (black line), and monomers (if the signal is strong enough to detect) and large aggregates have the weakest (green line).

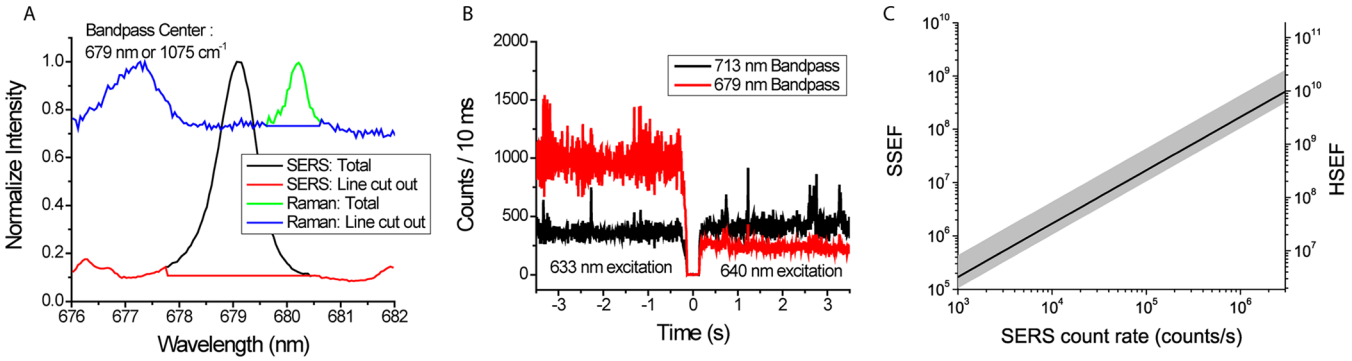

Figure 2. We calibrate the conversion of SERS count rate to enhancement factor by comparing strengths of Raman lines in SERS and confocal Raman measurements. (A) The fraction of signal monitored using a 679DF6 bandpass filter from the ring-breathing mode of MBA near 1080−1100 cm^{-1} is determined from the spectra. (B) We verify the determination of SERS signal fraction in part A by switching laser excitations. The laser excitation is switched by a flipper mirror at time 0 between a 633 nm HeNe laser and a 640 nm diode laser adjusted to have the same laser power (150 μW). The signal detected in the 679 nm bandpass goes down 70% due to the Raman band at 1080 cm^{-1} slipping out of the bandpass filter toward the red. The signal in the 713 nm filter is essentially unchanged, since no Raman line is present for the frequency range established by that bandpass filter. (C) The enhancement factor calibration determined for our measurements is shown in black. The possible range depending on the size of the hot spot regions is shown in gray. The left axis is for the SSEF, and the right axis is for the HSEF.

The range of enhancements that we find shows that the strategy of nanoparticle linking, encapsulation, and small molecule infusion provides a dependable way of preparing very bright SERS-active substrates for biomedical and other applications.

To determine whether or not a signal comes from an individual SERS hot spot, we performed correlation spectroscopy on nanocapsules undergoing free translational and rotational diffusion. SERS correlation spectroscopy[2,11] measures fluctuations in SERS signals caused by nanoparticle diffusion into and out of a confocal detection volume defined by a tightly focused laser excitation and a detection pinhole. The decay time scale of the correlation function measures the diffusion time across the confocal detection volume. Rotational diffusion of asymmetric nanoparticle dimers or multimers leads to an additional decay time scale corresponding to the rotational diffusion—a measure of the individual nanocapsule's rotational rate—with respect to the laser polarization axis; this time scale is typically shorter than the translational diffusion time scale (Figure 1C). Rotational diffusion decays can be measured in correlation spectroscopy only for nanocapsules with strong polarization responses. Aggregates or spherically symmetric nanoparticles only exhibit decays due to translational diffusion.[2]

Hot spots formed by interparticle junctions exhibit a very strong polarization response that can be monitored at the single particle level.[12] A strong polarization response strongly suggests that a single hot spot dominates the observed signal; the only alternative interpretation is that multiple hot spots are aligned in a linear multimer by chance. Electron microscopy shows linear aggregates larger than the dimer to be very rare; hence only the assumption that the observed highly polarization-sensitive SERS signals originate from a single dominant hot spot is probable. The excitation laser light was polarized, and

dx.doi.org/10.1021/nl3005447 | Nano Lett. 2012, 12, 2912−2917

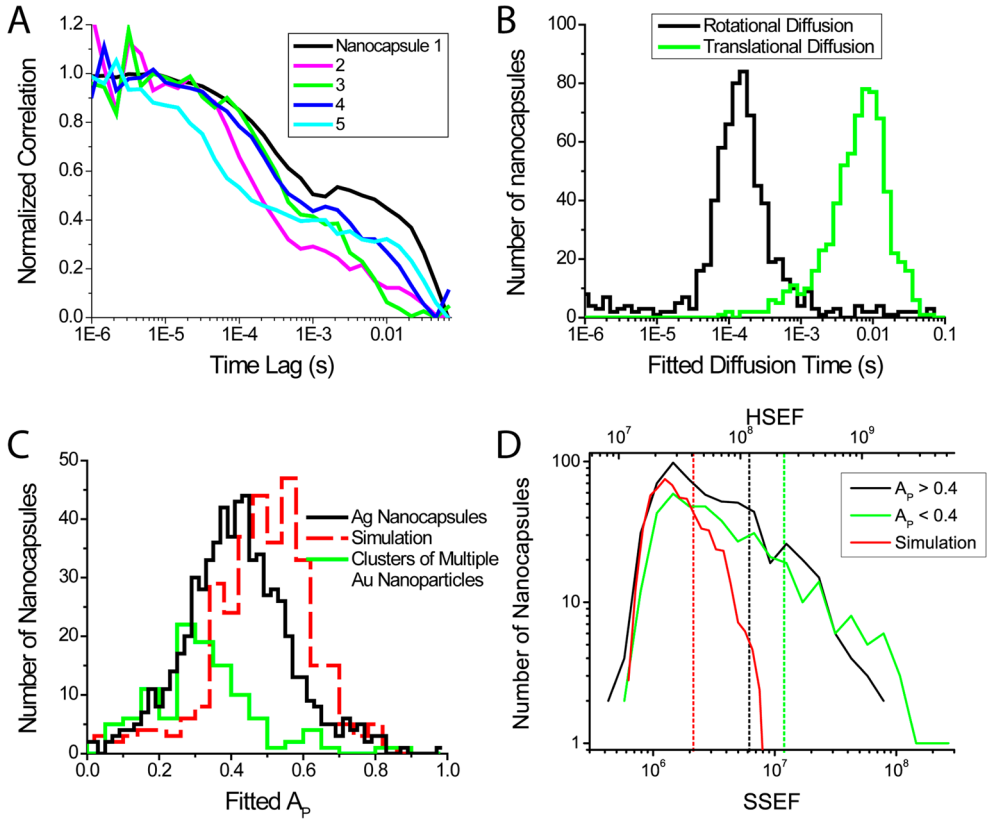

Figure 3. SERS enhancement factors for diffusing nanocapsules. (A) Correlation functions calculated for transits of individual nanocapsules. Rotational and translational diffusion time scales are visible. (B) Fitted rotational and translational diffusion time scales for individual nanocapsules. (C) Histogram of A_P, the fraction of total correlation amplitude, for measured nanocapsules (black) and simulated spherical dipole scattering centers (red) diffusing through a Gaussian detection volume. Green line shows distribution of A_P for clusters of multiple Au nanoparticles studied in ref 2. (D) Determined SERS enhancement factors (SSEF and HSEF) for individual hot spots selected for high rotational diffusion amplitude (A_P > 0.4; black line); the estimated values for low A_P (A_P < 0.4) are shown in green. A simulation of diffusing particles with a uniform excitation response (dotted red line) is shown. The dotted vertical lines indicate the average enhancement factors of the distributions with the corresponding colors.

our SERS correlation spectroscopy setup[2] measured both of the scattered components whose polarization is aligned with and perpendicular to the polarization of the exciting light. We selected nanocapsules where the fraction of the correlation amplitude arising from rotational diffusion, A_P, was higher than a threshold of 0.4 (see Supporting Information). This was the discriminating factor that allowed us to extract the signal originating primarily from single encapsulated nanoparticle dimers, rather than larger multimers.

We calculated SERS enhancement factors by comparing Raman signals of the 1080 cm^{-1} Raman band of MBA in methanol with the signals of the same Raman band from SERS nanocapsules. There may be a change in the Raman cross-section associated with the binding to the metal surface, especially since a shift of ~15 cm^{-1} in several Raman lines is observed. Although this adds some uncertainty in determining the enhancement factor in SERS, it ensures that the enhancement factors are only computed for MBA molecules bound to the Ag surface. We performed spectroscopy to identify Raman lines on one microscope[13] and determined absolute signal strengths on a separate microscope setup.[2] To determine intensities, we counted photons using avalanche photodiodes over narrow spectral ranges defined by bandpass filters rather than acquiring entire spectra. The nanocapsules were allowed to randomly diffuse through a detection volume defined by a tightly focused 633 nm excitation and confocal detection as described previously.[2] While sacrificing spectral information, this approach dramatically increases temporal resolution, allowing robust identification of the signal arising from an individual hot spot and acquisition of good quality measurements of intensity changes due to rotational diffusion.

Measurements of the intensity of a Raman line of MBA were performed on two high-concentration solutions of MBA in methanol (43 mM and 600 mM; e.g., Figure 2A, blue and green lines). The solutions were kept at 50 °C on a heating stage until used. The measurements were performed within two minutes to avoid MBA coming out of solution and completed before crystallization was visible.

The fraction of signal in the bandpass coming from MBA in solution, as determined by comparing the spectral line shapes (Figure 2A) to constant background levels, was f_{Raman} = 2.4% ± 1% for the fraction detected in Raman measurements and f_{SERS} = 56% ± 15% for the fraction detected in SERS measurements. Since the MBA signal occurs at a fixed wavenumber with respect to the excitation frequency, we verified the background signal by exciting with a second wavelength (640 nm; see Figure 2B), thereby shifting the SERS spectrum and leaving a featureless background signal in the bandpass wavelength range (covering 850−1000 cm^{-1} for 640 nm excitation).

In our comparison of Raman and SERS measurements, we account for the number of MBA molecules expected under excitation within a ~500 nm diameter excitation beam and the measured laser excitation intensities (150−600 μW). The effective detection volume of 2.8 ± 0.5 femtoliters was

dx.doi.org/10.1021/nl3005447 | Nano Lett. 2012, 12, 2912−2917

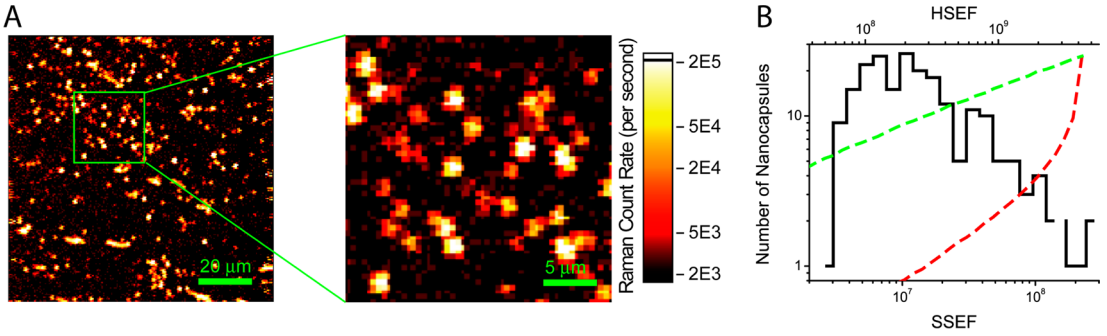

Figure 4. SERS enhancement factors for surface-immobilized nanocapsules. (A) Confocal scattering image. (B) Enhancement factors extracted for individual nanocapsules in (A). Dotted red line is the distribution expected for uniform sample with circular excitation polarization. Dotted green line is the distribution expected for uniform sample with linear excitation polarization.

determined by fluorescence correlation spectroscopy measurements on known concentrations of Alexa 647. $N_{Raman} = 1 \times 10^9 \pm 2 \times 10^8$ molecules of MBA were thus present in this detection volume for a concentration of 600 mM. The total intensity of this solution was measured to be $S_{Raman} = 8.2 \pm 0.1$ kHz, which corresponds to a signal strength $S_{Raman} f_{Raman}$ of 200 ± 70 Hz for the monitored Raman line.

We now estimate the average number of MBA molecules on a nanocapsule's surface which we use for computing SSEF and HSEF. In calculating the SSEF, we calculate the total average area of a nanocapsule. Based on the data from previous work,[1] the nanoparticle diameters range from 20 to 60 nm. Accounting for the distribution in the number of nanoparticles per nanocapsule (Figure 3a in ref 1) and the distribution in sizes, we calculate an average total surface area of 15 000 ± 9000 nm^2.

For the HSEF, we calculate the expected average hot spot area of a nanocapsule, which is associated with junctions between nanoparticles. Previous calculations found that the electric field enhancements are much stronger in the junctions and would dominate the SERS signal.[5,10] The strong polarization selectivity found here and elsewhere[12] is consistent with this structural picture. The TEM images taken of SERS nanocapsules (e.g., from ref 1) provided estimates (15 ± 4 nm diameter for 27 nanoparticle junctions) for the contact area between nanoparticles. Based on this, we estimate the areas of junctions between nanoparticles within the nanocapsules. Accounting for the number of nanoparticles in a nanocapsule, the area of contact (and presumably the hot spot area) would therefore range from 200 to 560 nm^2.

Assuming monolayer coverage of MBA on both surfaces[14] with a measured spacing of 0.8 × 0.8 nm, we expect 600−1800 MBA molecules for the hot spot(s) in a given nanocapsule and 9000−37 000 MBA molecules for the entire surface area of the nanocapsules. We used the average value N_{SERS} = 1200 molecules per hot spot in our HSEF calculations and an average value of N_{SERS} = 23000 molecules in our SSEF calculations, with approximately a 50% uncertainty due to area. These calculations assume monolayer coverage which may not be possible due to the polymer coating and linker groups on the surface of the nanoparticles; hence, the number of MBA molecules is likely smaller. The reported enhancement factors are, therefore, lower bounds of the larger actual enhancement factors.

We used SERS intensity measurements on the fast timing setup on freely diffusing nanocapules, the foregoing observations, and the following formula to calculate the SERS enhancement factor (EF):

$$EF = \frac{f_{SERS} S_{SERS}}{f_{Raman} S_{Raman}} \frac{I_{Raman}}{I_{SERS}} \frac{N_{Raman}}{N_{SERS}} \quad (1)$$

where I_{SERS} and I_{Raman} are the laser excitation intensities for the Raman and SERS experiments. The largest uncertainties in the values come from the estimated value used for the number of MBA molecules per nanocapsule or per SERS hot spot. An additional orientation factor of up to a value of 3 may be present, whose precise value depends on the degree of randomness of the adsorbed MBA with respect to the dimer's axis. The factor of 3 would be appropriate if the MBA is fully randomly oriented (Supporting Information).

Measurements of SERS line intensity and rotational diffusion-induced intensity fluctuations of individual freely diffusing nanocapsules were performed in 10 min experiments as described by Laurence et al.[2] (The Rayleigh scattering channel was eliminated for these measurements and the laser was linearly polarized.) It was previously shown that the polarization sensitivity of SERS leads to rotational diffusion-induced intensity fluctuations from nanoparticles randomly diffusing in aqueous solutions.[2,11] Correlation functions calculated on individual nanocapsules show two time scales:[2,15] a shorter, polarization sensitive time scale (100 μs; Figure 3B) due to rotational diffusion with respect to the excitation polarization and a longer time scale due to translational diffusion into and out of the detection volume (Figure 3A).

The relative magnitude of the rotational diffusion components as shown in Figure 3C (black line) indicates that the SERS intensity values measured are dominated by signals from one or a small number of hot spots. The distribution of A_P, the fraction of total correlation amplitude due to rotational diffusion, is very similar to that obtained from a simulation of 100 nm spherical particles which scatter preferentially along a single axis of polarization (red line, Figure 3C). The somewhat lower value of A_P observed (average of 0.4 A_P for the nanocapules vs 0.48 A_P for the simulation) is probably due to the presence of trimers, tetramers, and higher order multimers. By selecting only nanocapsules with high values of A_P >0.4 we select a nanocapsule subpopulation dominated by dimers with single hot spots. The distribution observed is in contrast to that observed for clusters of multiple Au nanoparticles studied in ref 2 (green line); larger aggregates and spherically symmetric particles (such as the hollow gold nanospheres in ref 2) show little or no polarization response, resulting in A_P values near 0.

The distribution of SERS enhancement factors computed from the diffusing nanocapsules using eq 1 are shown in Figure 3D. The SSEF values range from 10^6 and 10^8, and the HSEF

dx.doi.org/10.1021/nl3005447 | Nano Lett. 2012, 12, 2912−2917

values range from 2×10^7 to 2×10^9. Note that the nanocapsules with $A_P < 0.4$ had larger estimated enhancement factors, likely due to the presence of more than one hot spot. For $A_P > 0.4$, the average SSEF is 6×10^7, and average HSEF is 10^8 with ranges that are consistent with previously observed values in Ag nanoparticle junctions.[5,8] (The uncertainty in these values due to area considerations is approximately a factor of 2.) The simulation of freely diffusing particles with uniform response in a confocal detection volume (described in ref 16) in Figure 3D (dotted red line) is narrower than our measured enhancement factors. This suggests that the experimental distribution observed is dominated by variations in the nanocapsules rather than caused by the analysis.

In the measurements on freely diffusing nanocapsules, the varying diffusion paths the nanocapsules take through the detection volume contribute to the observed intensities and the distribution of enhancement factors observed. To verify that this is not the dominant source of the distribution observed, we measured enhancement factors of nanocapsules immobilized on a coverslip (in this measurement, we are not able to use rotational diffusion to distinguish between dimers and a higher-order multimers). As shown in Figure 4, we again see a rather wide distribution of enhancement factors. The slower rise in the distribution near the detection threshold (which for this case corresponded to SSEF = 3×10^6) shows that there is truly a peak in the enhancement factor distribution above 3×10^6, not just a continuously rising distribution below 3×10^6. In this experiment we used circular polarization for excitation to minimize effects of the highly polarized scattering response of the nanocapsules. However, we were not able to eliminate the possibility of alignment along the optical axis. If α is the angle of the dimer polarization with respect to the optical axis, then the observed intensity should vary as $\sin^4 \alpha$ (Supporting Information). A simple simulation based on this (dotted red line; Supporting Information) shows a distribution very different from the observed distribution. This result does not depend on having perfect circular polarization: Linear excitation polarization (dotted green line) still produces a distribution very different from the observed distribution.

Combining the information from the diffusing and immobilized nanocapsules, we find that the nanocapsules have SSEF values in the range from 10^6 and 10^8 and the HSEF values in the range from 2×10^7 to 2×10^9. These values are consistent with values previously determined in nanoparticle junctions.[5,8−10] The consistently high enhancement factors obtained show that the nanoparticle linking, and infusion of Raman-active tags is a dependable strategy for developing SERS-active substrates that can interact with the local chemical environment without aggregation.

These experiments use polarization sensitivity as a primary discriminant for determining the enhancing properties of a newly synthesized nanoparticle-based SERS substrate. The short 10 min collection times for these measurements on diffusing nanocapsules allow a statistically significant characterization of the EF distribution of a SERS-active mixture. Using rotational correlation spectroscopy measurements we were able to show that a single hot spot typically dominates the signal for each nanocapsule. We did not find a significant contribution from a population lacking a strong polarization response, even though monomer nanocapsules were plentiful. This implies that the observed SERS intensity originates overwhelmingly from nanocapsules containing two or more nanoparticles.

The measurements and analysis on correlations of single particles as performed here may be applied to the correlation spectroscopy of other oriented nanoparticles, such as semiconductor nanorods[17] and gold nanorods.[18] Rotational correlation spectroscopy on individual nanoparticles may be also applied toward eliciting other useful physical properties. For example, it may be used as a rotational probe for shear forces.

■ ASSOCIATED CONTENT

Supporting Information

Additional equations and description of simulations. This material is available free of charge via the Internet at http://pubs.acs.org.

■ AUTHOR INFORMATION

Corresponding Author

*E-mail: laurence2@llnl.gov

Author Contributions

§These authors contributed equally.

Notes

The authors declare no competing financial interest.

■ ACKNOWLEDGMENTS

This work performed under the auspices of the U.S. Department of Energy by Lawrence Livermore National Laboratory under contract DE-AC52−07NA27344. M.M. acknowledges support by the Institute for Collaborative Biotechnologies through grant DAAD19−03-D- 0004 from the U.S. Army Research Office.

■ REFERENCES

(1) Braun, G. B.; Lee, S. J.; Laurence, T.; Fera, N.; Fabris, L.; Bazan, G. C.; Moskovits, M.; Reich, N. O. *J. Phys. Chem. C* **2009**, *113*, 13622.

(2) Laurence, T. A.; Braun, G.; Talley, C.; Schwartzberg, A.; Moskovits, M.; Reich, N.; Huser, T. *J. Am. Chem. Soc.* **2009**, *131*, 162.

(3) Pallaoro, A.; Braun, G. B.; Reich, N. O.; Moskovits, M. *Small* **2010**, *6*, 618.

(4) Pallaoro, A.; Braun, G. B.; Moskovits, M. *Proc. Natl. Acad. Sci. U.S.A.* **2011**, *108*, 16559.

(5) Wustholz, K. L.; Henry, A. I.; McMahon, J. M.; Freeman, R. G.; Valley, N.; Piotti, M. E.; Natan, M. J.; Schatz, G. C.; Van Duyne, R. P. *J. Am. Chem. Soc.* **2010**, *132*, 10903.

(6) Goddard, G.; Brown, L. O.; Habbersett, R.; Brady, C. I.; Martin, J. C.; Graves, S. W.; Freyer, J. P.; Doorn, S. K. *J. Am. Chem. Soc.* **2010**, *132*, 6081.

(7) Fleger, Y.; Mastai, Y.; Rosenbluh, M.; Dressler, D. H. *Surf. Sci.* **2009**, *603*, 788.

(8) Le Ru, E. C.; Blackie, E.; Meyer, M.; Etchegoin, P. G. *J. Phys. Chem. C* **2007**, *111*, 13794.

(9) McFarland, A. D.; Young, M. A.; Dieringer, J. A.; Van Duyne, R. P. *J. Phys. Chem. B* **2005**, *109*, 11279.

(10) Talley, C. E.; Jackson, J. B.; Oubre, C.; Grady, N. K.; Hollars, C. W.; Lane, S. M.; Huser, T. R.; Nordlander, P.; Halas, N. J. *Nano Lett.* **2005**, *5*, 1569.

(11) Eggeling, C.; Schaffer, J.; Seidel, C. A. M.; Korte, J.; Brehm, G.; Schneider, S.; Schrof, W. *J. Phys. Chem. A* **2001**, *105*, 3673.

(12) Jiang, J.; Bosnick, K.; Maillard, M.; Brus, L. *J. Phys. Chem. B* **2003**, *107*, 9964.

(13) Talley, C. E.; Jusinski, L.; Hollars, C. W.; Lane, S. M.; Huser, T. *Anal. Chem.* **2004**, *76*, 7064.

(14) Schafer, A. H.; Seidel, C.; Chi, L. F.; Fuchs, H. *Adv. Mater.* **1998**, *10*, 839.

(15) Laurence, T. A.; Kwon, Y.; Yin, E.; Hollars, C. W.; Camarero, J. A.; Barsky, D. *Biophys. J.* **2007**, *92*, 2184.

(16) Laurence, T. A.; Kapanidis, A. N.; Kong, X. X.; Chemla, D. S.; Weiss, S. *J. Phys. Chem. B* **2004**, *108*, 3051.
(17) Tsay, J. M.; Doose, S.; Weiss, S. *J. Am. Chem. Soc.* **2006**, *128*, 1639.
(18) Tcherniak, A.; Dominguez-Medina, S.; Chang, W. S.; Swanglap, P.; Slaughter, L. S.; Landes, C. F.; Link, S. *J. Phys. Chem. C* **2011**, *115*, 15938.